LA-UR-01-4821
Approved for public release; distribution is unlimited.

Title: **Ultrafast Optical-Pump Terahertz-Probe Spectroscopy of Strongly Correlated Electron Materials**

Author(s): R. D. Averitt, V. K. Thorsmølle, A. I. Lobad, Q. X. Jia S. A. Trugman and A. J. Taylor

Submitted to:

http://lib-www.lanl.gov/la-pubs/00796336.pdf

Ultrafast Optical-Pump Terahertz-Probe Spectroscopy of Strongly Correlated Electron Materials

R. D. Averitt [a,*] V. K. Thorsmølle [a] A. I. Lobad [b] Q. X. Jia [a]
S. A. Trugman [a] A. J. Taylor [a]

[a] *Los Alamos National Laboratory, Los Alamos, NM 87545*
[b] *Kirtland AFB-DELS, Albuquerque, NM 87117*

Abstract

We have used optical-pump far-infrared probe spectroscopy to probe the low energy electron dynamics of high temperature superconductors and colossal magnetoresistance manganites. For the superconductor $YBa_2Cu_3O_7$, picosecond conductivity measurements probe the interplay between Cooper-pairs and quasiparticles. In optimally doped films, the recovery time for long-range phase-coherent pairing increases from ~1.5 ps at 4K to ~3.5 ps near T_c, consistent with the closing of the superconducting gap. For underdoped films, the measured recovery time is temperature independent (3.5 ps) in accordance with the presence of a pseudogap. Ultrafast picosecond measurements of optically induced changes in the absolute conductivity of $La_{0.7}M_{0.3}MnO_3$ thin films (M = Ca, Sr) from 10K to ~$0.9T_c$ reveal a two-component relaxation. A fast, ~2 ps, conductivity decrease arises from optically induced modification of the effective phonon temperature. The slower component, related to spin-lattice relaxation, has a lifetime that increases upon approaching T_c from below in accordance with an increasing spin specific heat. Our results indicate that for $T<<T_c$, the conductivity is determined by incoherent phonons while spin fluctuations dominate near T_c.

Key words:
ultrafast, superconductivity, terahertz, manganite

* Los Alamos National Lab, MST-10 Condensed Matter and Thermal Physics, MS K764, Los Alamos, NM 87544 Phone: (505) 667-1644 Fax: (505) 665-7652, Email: raveritt@lanl.gov

1 Introduction

One of the primary goals of contemporary materials physics is to understand and control phenomena in which the dynamics of electrons are locally influenced by other electrons. This local influence includes Coulomb repulsion and exchange effects. When these effects become comparable in magnitude to the electron kinetic energy the results are dramatic and varied. Examples include superconductivity, and negative magnetoresistance. While a fundamental understanding of such phenomena is desirable, the stakes are also high from a technological perspective. Many "correlated electron" materials have potential applications including magnetic recording and, more generally, in the emerging field of spin electronics [1].

Ultrafast optical experiments can help elucidate the properties of correlated electron materials by resolving the dynamics in the time domain with 100-fs resolution. All-optical pump-probe experiments have displayed sensitivity to the low energy excitations in solids. However, following optical excitation, it would be advantageous to directly probe such low energy excitations. This has been made possible by combining terahertz time domain spectroscopy with synchronous optical excitation. Terahertz pulses are generated via optical rectification in ZnTe providing a coherent far-infrared source (containing Fourier components from 100 GHz to 2.5 THz). Measuring the optically induced changes in transmission of the THz pulses determines the conductivity dynamics with picosecond resolution. Several groups have been developing this technique, termed time-resolved THz spectroscopy (TRTS), to study various systems including photogenerated electrons in liquids such as hexane, or semiconductors such as GaAs [2,3]. We have utilized this technique to study high-T_c superconductors and "colossal" magnetoresistance manganites [4,5].

2 $Y_{1-x}Pr_xBa_2Cu_3O_{7-\delta}$ Thin Films

In high-T_c materials, optical pump-probe studies (with 1.5 eV photons) have been successfully employed to probe the superconducting gap and pseudogap [6]. The recovery of $\Delta R/R$ (R = reflectivity) on a picoseond timescale suggests that the superconducting pair recovery is rapid (with the rate-limiting step, as an example, possibly being due to the anharmonic decay of phonons). Recent experiments (1.5 eV) on single crystal YBCO have suggested an alternative interpretation of the dynamics - quasiparticle thermalization rather than pair recombination which is suggested to be much slower [7]. Using TRTS, we have directly measured the superconducting pair recovery demonstrating that the recovery following optical excitation does occur on a picosecond timescale (at least for our films, which do, however, have a substantially higher impurity

concentration than the single crystals in [7]).

Figure 1(a) and (b) show the conductivity as a function of frequency at 60K and 95K respectively (T_c = 89K) for a near optimally doped film. The phenomenological two-fluid model fits the data quite well (shown as a dashed line in Fig. 1(a)) below T_c where the imaginary conductivity is dominated by the $1/\omega$ dependence of the superfluid [4,8]. Above T_c, a standard Drude model fits the data (dashed line, Fig. 1(b)). Upon optical excitation, there is a decrease in the imaginary conductivity due to superconducting pair breaking with a corresponding increase in the real component (not shown). The induced change in $\sigma_{im}(\omega)$ is shown at 60K in figure 1(c). There is a decrease that rapidly recovers on a ps timescale that is due in large part to superconducting pair reformation. Figure 1(d) shows the induced change in $\sigma_{im}(\omega)$ at 95 K (above T_c) which is due quasiparticle relaxation.

The dynamics can be quantified by fitting the induced change in the imaginary conductivity as a function of time at a specified frequency. For optimal doping, the lifetime at 20 K is about 1.5 ps (at 1.0 THz) increasing to 3.0 ps near T_c. Above T_c, the lifetime of $\sigma_{im}(\omega)$ (which is no longer a measure of the superconducting recovery time, but rather the initial quasiparticle cooling) drops to 1.5 ps. In contrast, for $Y_{0.7}Pr_{0.3}Ba_2Cu_3O_7$ films (T_c = 50K) the lifetime is $\sim$3.5 ps independent of temperature even above T_c. This lifetime is the same as that measured in our undedoped $YBa_2Cu_3O_{6.5}$ films. These results suggest that for the optimally doped films, the dynamics are influenced by the closing of the superconducting gap, and that for the underdoped films, the pseudogap plays a role in determining the observed dynamics. Importantly, by directly measuring the dynamics associated with the imaginary conductivity, we have directly observed that the superconducting state does recover on a picosecond timescale.

3 $La_{0.7}M_{0.3}MnO_3$, M = Ca, Sr Thin Films

Manganese perovskites contain octahedrally coordinated manganese ions having a valence, when doped, that fluctuates between 3^+ and 4^+. These mixed-valence oxides are of the form $R_{1-x}D_xMnO_3$ where R is a trivalent rare earth and D is a divalent alkali. The materials have an extremely rich phase diagram including charge-ordering transitions, (anti-)ferromagnetism, and metal-insulator transitions, as well as a great sensitivity to small external perturbations such as pressure, magnetic field, chemical substitution [9,10]. The lattice and orbital degrees of freedom are also important in determining the electronic properties of colossal magnetoresistance manganites (CMR) materials above and below T_c. In the insulating paramagnetic regime, i.e. $T > T_c$, charge conduction proceeds via thermal activation of adiabatic small polarons [11]. In the

ferromagnetic regime the marginally-metallic conductivity of CMR materials suggests that overlapping large itinerant polarons are the conducting entities. We have used TRTS to study CMR materials with a view towards understanding the correlation between charge dynamics and orbital and magnetic structure.

Using TRTS the temporal evolution of the optically induced change in the absolute conductivity (at 0.7 THz) is plotted in Figs. 2(a) for $La_{0.7}Ca_{0.3}MnO_3$ (LCMO) and 2(b) for $La_{0.7}Sr_{0.3}MnO_3$ (LSMO) films. Two components characterize the conductivity dynamics: a fast, resolution-limited (<2 ps) response whose relative magnitude decreases as the temperature is increased and a slow component whose relative magnitude and time constant increases with increasing temperature. The fast component corresponds to electron-phonon equilibration and the slow component to spin-lattice thermalization. The plateau in the conductivity at longer times corresponds to equilibrium between the electrons, spins and phonons at a higher temperature than before the arrival of the pump.

To understand the measured dynamics, we consider a two-temperature model where the spins and the lattice are coupled subsystems having well defined temperatures T_s and T_l, respectively. Below T_c, the initial highly excited electronic state has shed its excess energy and thermalized via electron-phonon interactions during the first two picoseconds following excitation. The evolution of $\Delta T_{sl} = T_l - T_s$, subsequent to this initial electron-phonon equilibration, is governed by:

$$d\Delta T_{sl}/dt = -\Delta T_{sl} G_{sl}/b, \tag{1}$$

where G_{sl} is the spin lattice coupling constant and $b = C_s C_l/(C_s + C_l)$ with the spin and lattice specific heat given by C_s and C_l respectively. The spin-lattice relaxation process corresponds to spin reorientation proceeding via the combined effects of spin-orbit coupling and momentum scattering. The spin-lattice relaxation time can be estimated by $\tau_{sl} = b/G_{sl} \approx C_s/G_{sl}$. Heat conduction terms are ignored since they are weak and are relevant only on the nanosecond timescales.

Figures 3(a) and 3(b) show the measured lifetimes of the spin lattice relaxation time τ_{sl} as a function of temperature for LCMO and LSMO using the TRTS data of Figs. 2. The solid lines are fits from numerically solving Eq. 1 using the specific heat data of [12] (LCMO) and [13] (LSMO). These fits yield a temperature independent value of G_{sl} of 2.5×10^{15} (5×10^{15}) W/(m^3K) for LCMO (LSMO). Therefore, the calculated values of τ_{sl} in Figure 3 are proportional to the magnetic specific heat C_s, indicating that τ_{sl} exhibits the same temperature dependence as C_s. This behavior of τ_{sl} is a reflection of the interdependence in the manganites of the charge and spin degrees of freedom.

Further analysis of these experiments have allowed us to determine the relative influence of thermally disordered phonons versus spin disorder in determining the conductivity. In particular, at low termperatures ($T<<T_c$) thermally disordered phonons limit the conductivity while closer to T_c spin disorder limits the conductivity [5].

In conclusion, we have used optical-pump far-infrared probe spectroscopy to study the electron dynamics in high-T_c superconductors and CMR materials. We expect this technique to find application in the study of many other novel correlated electron materials.

References

[1] *Spin Electronics*, M. Ziese, M. J. Thornton editors (Springer-Verlag, Berlin 2001).

[2] E. Knoesel, M. Bonn, J. Shan, T. F. Heinz, Phys. Rev. Lett. 86 (2001) 340.

[3] M. C. Beard, G. M. Turner, C. A. Schmuttenmaer, Phys. Rev. B 62 (2000) 15764.

[4] R. D. Averitt, G. Rodriguez, J. L. W. Siders, S. A. Trugman, A. J. Taylor, Phys. Rev. B 63 (2001) 140502(R).

[5] R. D. Averitt, A. I. Lobad, C. Kwon, S. A. Trugman, V. K. Thorsmølle, and A. J. Taylor, Phys. Rev. Lett. 87 (2001) 017401.

[6] J. Demsar, B. Podobnik, V. V. Kabanov, T. Wolf, D. Mihailovic, Phys. Rev. Lett. 82 (1999) 4918.

[7] G. P. Segre, N. Gedik, J. Orenstein, D. A. Bonn, R. Liang, W. N. Hardy, cond-mat/0107325 (2001).

[8] S. D. Brorson, et al., J. Opt. Soc. Am. B 13 (1996) 1979.

[9] A. J. Millis, Nature 392 (1998) 147.

[10] *Colossal magneto-resistive oxides*, editor Y. Tokura, Gordon and Breach, Amsterdam, (2000).

[11] M. Jaime, et al., Phys. Rev. B 60 (1999) 1028.

[12] A. P. Ramirez, et al., Phys. Rev. Lett. 76 (1996) 3188.

[13] M. N. Khlopkin, et al., Phys. Solid State 42 (2000) 114.

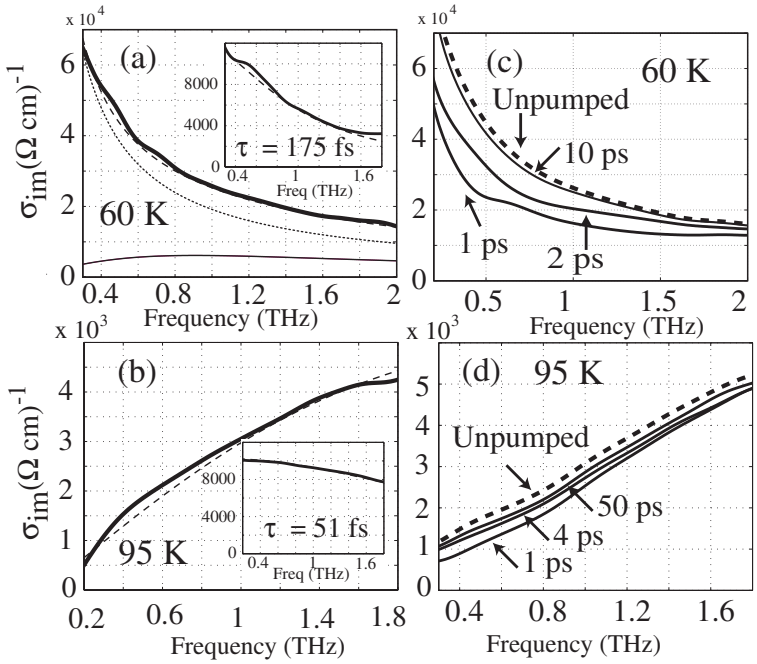

Fig. 1. (a)-(b) Conductivity at 60K and 95K, respectively for $YBa_2Cu_3O_7$. The imaginary conductivity is plotted with the real conductivity in the insets. The data is fit using a two-fluid model which reduces to the Drude model above T_c [4,8]. The thick solid line is the experimental data. The dashed lines are the overall fit to the data. In (a), the dotted line is the superconducting pair component and the thin solid line is the quasiparticle component. (c)-(d) Optically induced changes in the imaginary conductivity at 60 and 95 K.

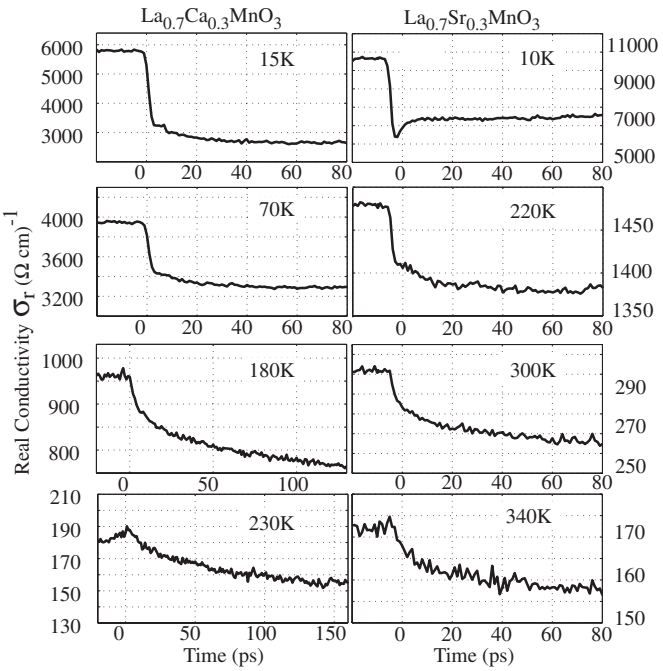

Fig. 2. Optically induced changes in the conductivity at 0.7 THz for LCMO and LSMO.

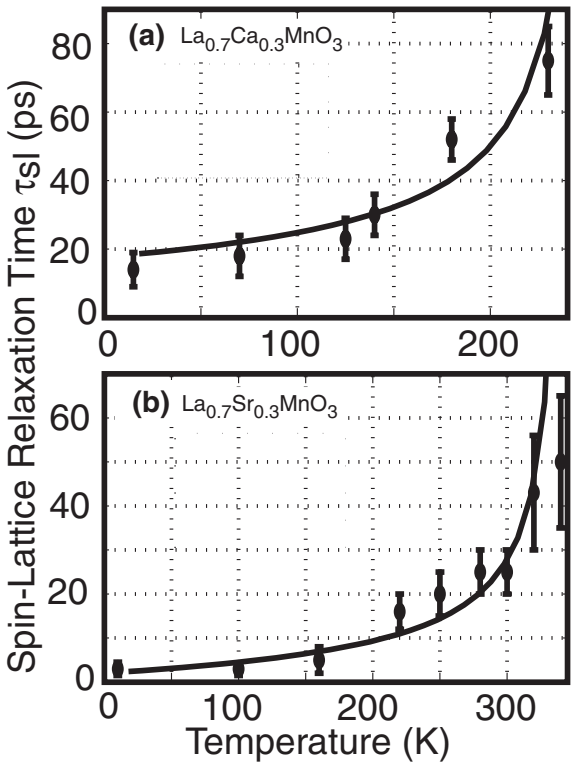

Fig. 3. Spin-lattice relaxation times from THz conductivity dynamics. The solid lines are calculations treating the spins and lattice as coupled subsystems.